PAPER ID: 1998583

Application of Compressional and Shear Slowness Overlay Technique in Identification of Low Resistivity & Low Contrast (LRLC) Pay Sands of Tipam Sandstone Reservoirs in Upper Assam Basin, India

Pradyut Bora, J. Phukan, R. Devi and S. K. Jena

Oil India Limited, Geology & Reservoir Department, Duliajan-786602, Assam, India

Presenting author, E-mail: pradyutbora@gmail.com

Abstract

The Upper Assam Basin is a matured petroliferous basin where commercial hydrocarbon has been established in clastic reservoirs of Tertiary sequence. The shallower fluvial Tipam sands of Miocene age was deposited in braided river system with a very good vertical and areal extent. Since, the Tipams have been deposited in a freshwater environments, identification and evaluation of hydrocarbon pays based on basic petrophysical logs is always challenging. Pay zones within Tipam Sandstone primarily exhibit low resistivity and low contrast (LRLC) nature on electrologs in most of the wells. As a result, apart from identification, there are uncertainty of fluid contacts, in-place hydrocarbon volume estimation leading to uncertainty for development planning of these reservoirs.

An approach of compressional (P-wave) & shear (S-wave) slowness overlay technique along with compressional to shear wave velocities (VpVs) ratio have been analyzed in wells with low resistivity & low contrast pay zones in Tipam formations located in various parts of the basin. This technique has proven to be useful hydrocarbon detection technique for Tipam sands and reduce the possibility of misinterpretation of any productive zone. The analysis revealed that gas or light hydrocarbon bearing zones can be easily identified by VpVs ratio plot, irrespective of there resistivity values. Based on the study, a few of the identified zones were tested and proved to be hydrocarbon bearing. Identification of those elusive pay zones along with fluid contacts, resulted in increase of reserve.

Introduction

The Upper Assam basin is a composite foreland basin which is located between the eastern Himalaya foot hills and the Assam-Arakan thrust belt and situated at the north-eastern corner of Indian Sub-continent. The wells under study are mainly confined to the OIL's operational area to the south bank of Brahmaputra River. The pay zones within shallower fluvial Tipam sandstone of Miocene age of Tertiary sequence exhibits low resistivity & low contrast (LRLC) nature on electrologs in many producing fields. Moreover, gamma-ray and density-neutron logs are also not very diagnostic in Tipam formations. The LRLC characteristics of Tipam Formation are attributed to presence of the higher fraction of silt sized particles, authigenic smectite clay-coated grains & presence of conductive minerals etc. Hence, identification of hydrocarbon pays based on basic petrophysical logs is always challenging & insufficient to detect and distinguish pay zones from water bearing zones.

Compressional (DTCo) & shear (DTSm) wave slowness data derived from processing of Dipole Shear Sonic log data is often used as an additional tool in identification of conventional hydrocarbon bearing zone, fluid contact & fluid type etc. To address the challenges of identification of LRLC pay zones, application of these acoustic log data has been analyzed for unconventional LRLC Tipam sandstone reservoirs. Compressional and shear wave slowness in combination, either as overlay or ratio has been successfully used in identification of LRLC Tipam pay zones and proved to be useful. This paper deals with the application of compressional and shear slowness overlay technique in the identification of LRLC Tipam pay sands with field examples. Adoption of this technique has also been observed to be useful where the gamma ray log and density-neutron overlay are not very diagnostic. Production testing and fluid identification by wireline conveyed Formation Tester results of a few sands has validated the application of these techniques.

Dipole shear sonic measurements in identification of Low resistivity & Low contrast pay zones

Dipole Shear Sonic logging tool is now widely used in the industry as it is capable of measuring high quality shear, compressional, stoneley slowness data in both hard and soft formations. This advancement of sonic technology delivers invaluable data for identification of rock mechanical properties, porosity, fluid type, assist seismic interpretation and geo-mechanical studies. Utilizing the well-understood effect of gas on acoustic results, it is also possible to identify low resistivity pay in unconsolidated sands where resistivity contrast is small.

In sand bodies, acoustic velocities are dependent on rock matrix, porosity, mineralogy, grain to grain contacts, type of fluid and degree of consolidation. It is well known from previous research work that the acoustic velocities can always be expressed in terms of moduli that are intrinsic measures of rock frame and pore fluid compressibility. In elastic and isotropic medium the compressional (Vp) and shear (Vs) wave velocities are related to the dynamic elastic moduli with the following relations.

$Vp = \sqrt{(K + 4/3\ G)\rho_b}$ -----------Equ(1)

$Vs = \sqrt{G/\rho_b}$ ---------------------Equ(2)

Where, Vp and Vs are compressional and shear wave velocities, expressed in km/sec.

K and G are bulk modulus and shear modulus, expressed in GPa (Giga Pascals)

ρ_b is the bulk density in g/cc (matrix, fluid and porosity combined).

Compressional wave velocity is sensitive to the saturating fluid type and depends upon formation compressibility, where as shear wave velocity depends upon formation rigidity. In unconsolidated sands, the replacement of water saturating fluid, which has very large bulk modulus by light hydrocarbon, which is highly compressible, is known to have a strong influence on compressional wave slowness. In the presence of light hydrocarbon, the increase of compressional slowness (decrease of compressional wave velocity) is due to the overall decrease of bulk modulus (K) of reservoir rocks which strongly depends on the bulk-fluid modulus, whereas the shear does not. Presence of gas reduces the rock rigidity more than its density and this reduction will dominate the compressional velocity (Vp) and, according to Equ-(1), it will decrease. The decrease in compressional wave velocity is almost nil in low porosity formations where pore volume is low and compaction pressure is high which means pore fluid contributes little to rock rigidity. In high porosity formations where pore volume is large and compaction pressure is less, the pore fluid has a much larger contribution to the rock rigidity. However, for a shear wave, if water is exchanged for light hydrocarbon, its velocity increases slightly according to Equ-(2) above. As shear velocity is relatively independent of fluid type, so there is no appreciable hydrocarbon effect on the shear modulus (G), unlike the compressional wave. Thus the net effect on compressional to shear wave velocities (Vp/Vs) if water in the pore space is replaced with gas is that it will decrease.

Techniques of LRLC payzone identification

In this study, compressional and shear slowness overlay technique has been used in identification of LRLC pay zones. In this technique, both the compressional (DTCo) and shear (DTSm) slowness log curves has been overlayed against known water saturated sand zone, than the overall variation of these two log curves analyzed in the rest of the reservoir rocks. The compressional slowness increases when the water saturated points become light hydrocarbon saturated points, while shear slowness is insensitive to the formation fluid in the pore space. Hence, presence of hydrocarbon causes mark separation between compressional and shear slowness log curves display against hydrocarbon bearing sand zones. Additionally, VpVs ratio and crossplot of VpVs ratio vs DTCo (compressional slowness) has also been utilized to assist the interpretation. The saturating fluid type can be identified by analyzing the variation of VpVs ratios. In light hydrocarbon bearing zones VpVs ratio decreases, whereas in water bearing zones the ratio increases. The cross-plot of VpVs ratio along Y-axis and compressional wave slowness along X-axis has been used after plotting on the standard template. Presence of hydrocarbon causes decrease in VpVs ratio with respect to water saturated point. Hence, the points corresponding to the hydrocarbon bearing zones tend to show a south-easterly trend on the cross-plot. Presence of dry/ light gas causes more departure of corresponding points from water saturated line towards south.

Results & Discussions

The above techniques have been successfully applied for identification both conventional and unconventional (LRLC) hydrocarbon bearing zones in many wells. Few case studies are presented below for both proved and identified wells showing how those techniques has been used to detect and distinguish water from gas (or light oil) saturated zones having LRLC characteristics.

i) **Well-A** : Resistivity of the highlighted sand zone is 5-7 ohm.m. and lower water bearing zone is 6-10 ohm.m. After overlaying DTCo and DTSm in the lower tested water bearing zone, significant separation observed between DTCo & DTSm in the highlighted zone due to the presence of light hydrocarbon. The highlighted zone exhibits VpVs ratio of about 1.8 and water bearing zone exhibits about 2. VpVs vs DTCo crossplot shows southward trend of values (black circle) corresponding to the highlighted zone. During production testing of the highlighted zone, the zone produced gas @ 71,000 standard cubic meters per day (scumd). Total pay thickness is about 13 m. (refer **Figure-1**).

ii) **Well-B** : Resistivity of the highlighted sand zone is 8-20 ohm.m. and adjacent water leg is 13-16 ohm.m. After overlaying DTCo and DTSm in the water bearing zone, significant separation observed between DTCo & DTSm in the highlighted zones due to the presence of light hydrocarbon. The highlighted zones exhibits VpVs ratio of about 1.74 and adjacent water leg exhibits about 2. VpVs vs DTCo crossplot shows southward trend of values (black circle) corresponding to the highlighted zone. During production testing of the highlighted zone, it produced gas @ 50,000 scumd. Total pay thickness is about 25 m. (refer **Figure-2**).

iii) **Well-C** : Resistivity of the highlighted sand zone is 8-15 ohm.m. and adjacent water leg is 8-10 ohm.m. After overlaying DTCo and DTSm in the water bearing zone, minor separation observed between DTCo & DTSm in the top highlighted zone. Difference of VpVs ratio also observed between highlighted and adjacent water leg. The highlighted zone exhibits VpVs ratio of about 1.6 and adjacent water leg exhibits VpVs ratio of about 1.75. VpVs vs DTCo crossplot also shows southward trend of values (black circle) corresponding to the highlighted zone. During production testing of the highlighted zone, it produced oil @ 4 klpd (Gas oil ratio: 3537 scum/kl) with 2 klpd water. (refer **Figure-3**).

iv) **Well-D** (Zone-1): Resistivity of the highlighted sand zone is 8-18 ohm.m. and adjacent water leg is 8-9 ohm.m. After overlaying DTCo and DTSm in the water bearing zone, significant separation observed between DTCo & DTSm in the highlighted zone due to the presence of light hydrocarbon. The highlighted zone exhibits VpVs ratio of about 1.8 and water leg exhibits about 2. VpVs vs DTCo crossplot shows southward trend of values corresponding to the highlighted zone (black circle). Fluid contact is prominent in DTCo and DTSm overlay, which is misleading in conventional tripple combo logs. Fluid identification was also performed by analyzing optical fluid analyzer responses (LFA) through wireline conveyed formation tester. Optical fluid analysis performed at middle and near the fluid contact of highlighted zone identified gas and volatile oil respectively in the flowline. Total pay thickness is about 22 m. (refer **Figure-4**).

v) **Well-D** (Zone-2): The resistivity of highlighted zone is around 6-10 ohm.m. and adjacent water leg is 8-11 ohm.m. After overlaying DTCo and DTSm in the water bearing zone, separation observed between DTCo & DTSm in the highlighted zone. The highlighted zone exhibits VpVs ratio of about 1.82 and adjacent water leg exhibits about 2. VpVs vs DTCo crossplot shows southward trend of values (black circle) corresponding to the highlighted zone. Based on the analogous response of DTCo & DTSm as above proved zones, the highlighted zone is identified to be light hydrocarbon bearing. Total pay thickness is about 13 m. (refer **Figure-5**)

vi) **Well-E** : The resistivity of highlighted zone is around 15-20 ohm.m. and comparable to adjacent water leg. After overlaying DTCo and DTSm in the water bearing zone, significant separation observed between DTCo & DTSm in the highlighted zone. The highlighted zone exhibits VpVs ratio of about 1.6-1.8 and adjacent water leg exhibits about 1.9-2. VpVs vs DTCo crossplot shows southward trend of values (black circle) corresponding to the highlighted zone. Side wall core samples shows bluish white fluorescence. Based on the analogous response of DTCo & DTSm as proved zones, the highlighted zone is identified to be light hydrocarbon bearing. Total pay thickness is about 23 m. (refer **Figure-6**)

vii) **Well-F** : The resistivity of highlighted zones are around 9-19 ohm.m. and adjacent water leg is 20-23 ohm. m. After overlaying DTCo and DTSm in the water bearing zone, significant separation observed between DTCo & DTSm in the highlighted zones. The highlighted zone exhibits VpVs ratio of about 1.6-1.8 and adjacent water leg exhibits about 1.9-2. VpVs vs DTCo crossplot shows southward trend of values (black circle) corresponding to the highlighted zone. The highlighted zones are identified to be light hydrocarbon bearing. Total pay thickness is about 7 m. (refer **Figure-7**).

Conclusions

Identification of low resistivity & low contrast pay zones for Tipam sands are quite challenging by analyzing resistivity response only and can lead to erroneous conclusions. Compressional & shear slowness overlay technique is effectively used for identification of LRLC pay zones along with fluid contacts, irrespective of their resistivity values. The acoustic gas effect is most pronounced in younger & unconsolidated LRLC Tipam sands. Additionally, VpVs ratio and cross-plots has also been found useful in the analysis. In spite of low resistivity, gas bearing zones has been easily identified by VpVs ratio plot. Minimum VpVs ratio of gas/light hydrocarbon bearing zones of presented examples is 1.6; however VpVs ratio appeared to be subjective in individual zone to set a definite cut-off limit for distinguishing hydrocarbon from water bearing zone. These techniques have been invariably applied apart from conventional log interpretation of triple combo logs to reduce the possibility of misinterpreting any productive zone. These techniques has also been found to be useful where the gamma ray and neutron-density logs are not very diagnostics. Identification of those elusive pay zones along with fluid contacts, has resulted in increase of reserve.

References

Hamada, G.M., 2004, Reservoir fluids identification using Vp/Vs ratio. Oil & Gas Science and Technology – Rev. IFP, Vol. 59, No. 6, pp. 649-654.

Brie, A., Mueller, M. C., Codazzi, D., Plona, T., Oil Field Review-New directions in sonic logging, Spring 1998, pp. 40-55.

Rao, R. V., Dependence of Vp/Vs vs. DTc crossplot technique for Gas-Water identification on degree of compaction and effective stress. 5th Conference & Exposition on Petroleum Geophysics, Hyderabad-2004, India, pp. 167-169.

Bahremandi, M., Mirshahani, M. and Saemi, M., Using of compressional-wave and shear-wave velocities ratio in recognition of reservoir fluid contacts-case study: A Southwest Iranian oil field. Journal of Scientific Research and Reviews Vol. 1(2), pp. 15 - 19, August 2012.

O. Chardac, Brie, A., Chouker, A. C., Correlations of Shear vs. Compressional in Shaly Sands and Application to Quicklook Hydrocarbon Detection. SPE 84205. SPE Annual Technical Conference, Denver, Colorado, U.S.A., 5 – 8 October 2003.

Figures

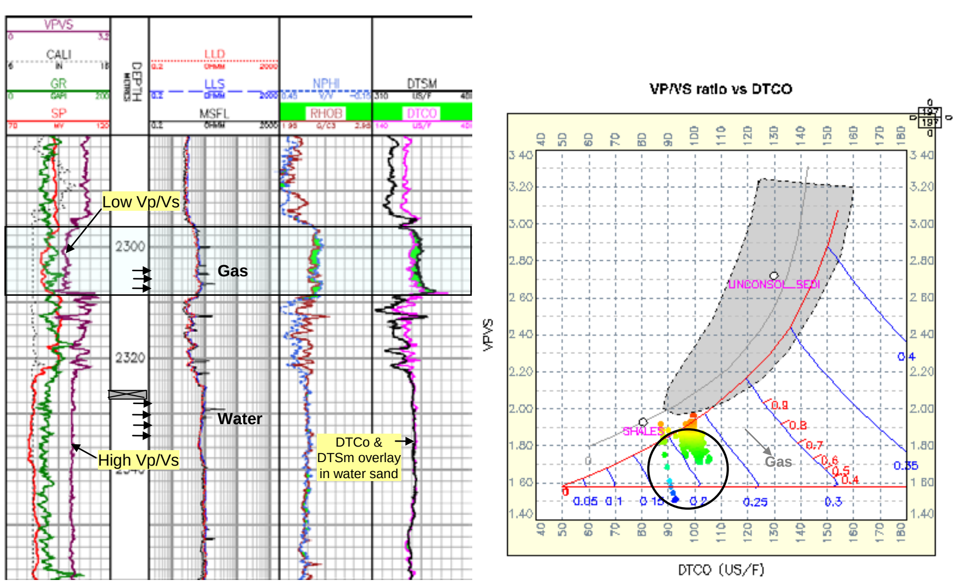

Figure-1: Well-A: DTCo & DTSm overlay and VpVs vs DTCo crossplot.

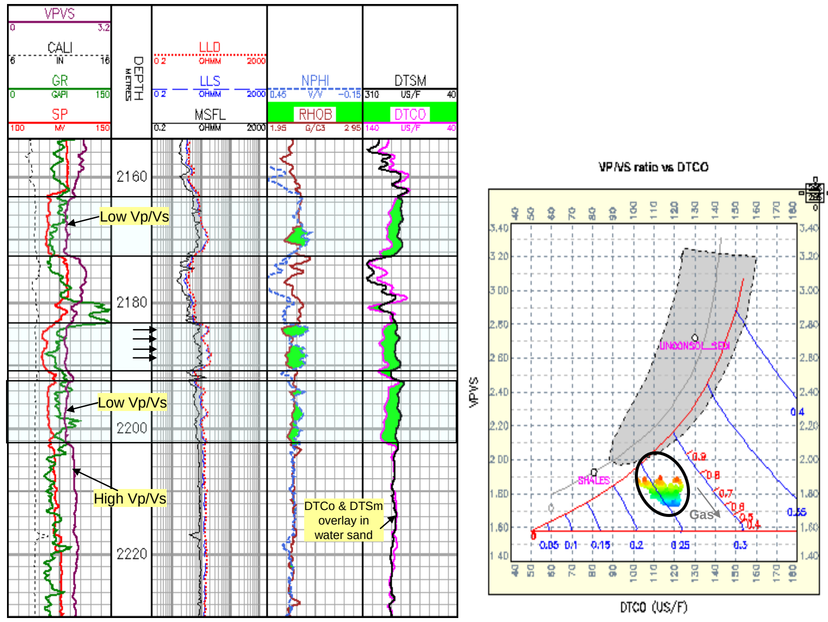

Figure-2: Well-B: DTCo & DTSm overlay and VpVs vs DTCo crossplot.

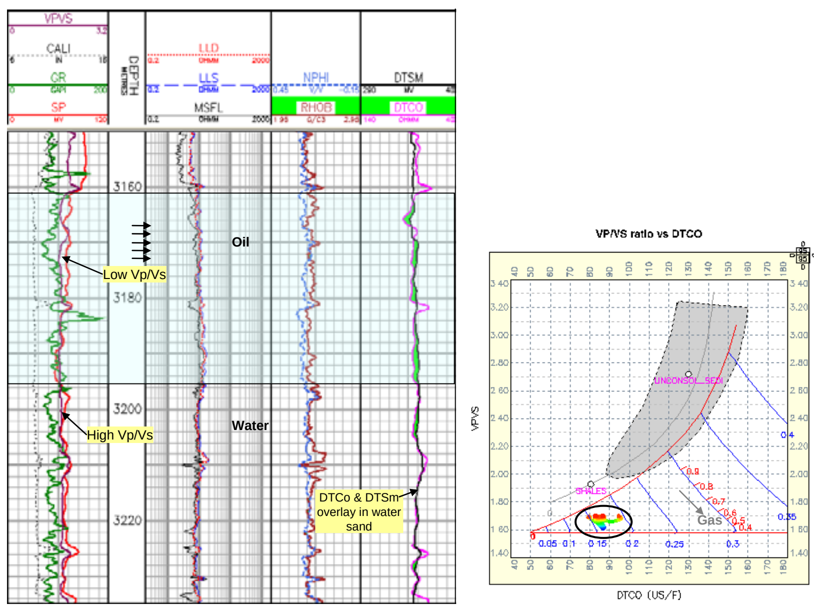

Figure-3: Well-C: DTCo & DTSm overlay and VpVs vs DTCo crossplot.

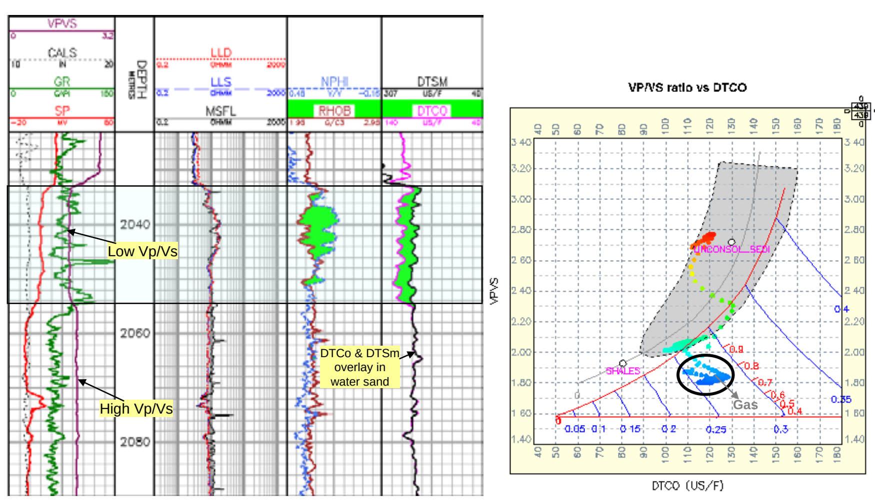

Figure-4: Well-D (Zone-1): DTCo & DTSm overlay and VpVs vs DTCo crossplot.

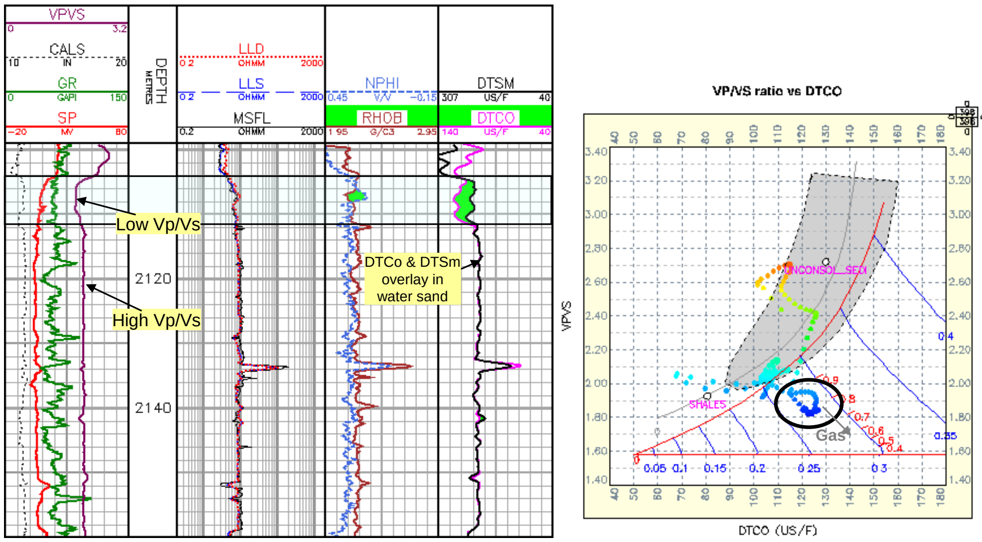

Figure-5: Well-D (Zone-2): DTCo & DTSm overlay and VpVs vs DTCo crossplot.

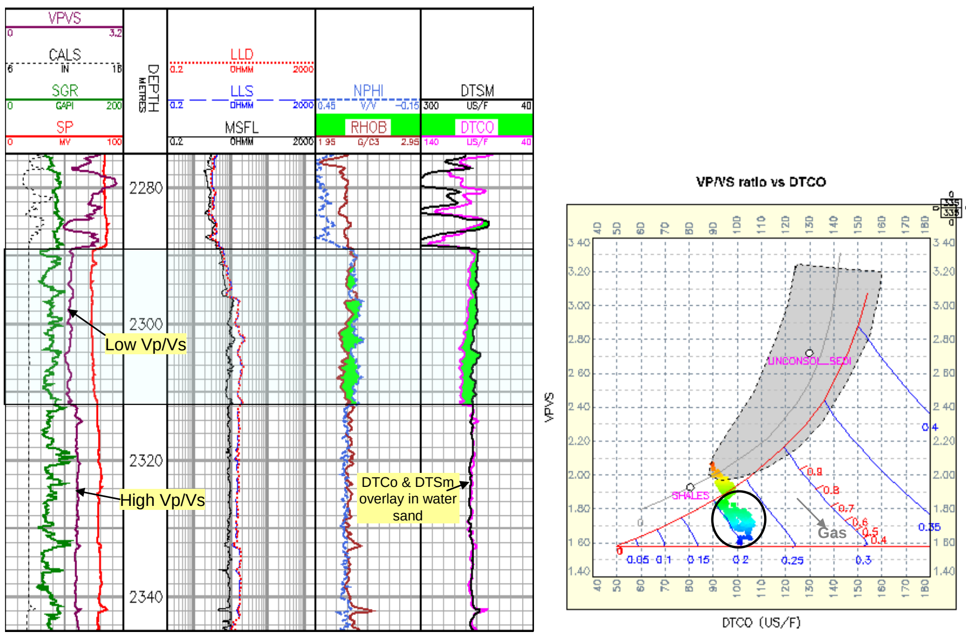

Figure-6: Well-E: DTCo & DTSm overlay and VpVs vs DTCo crossplot.

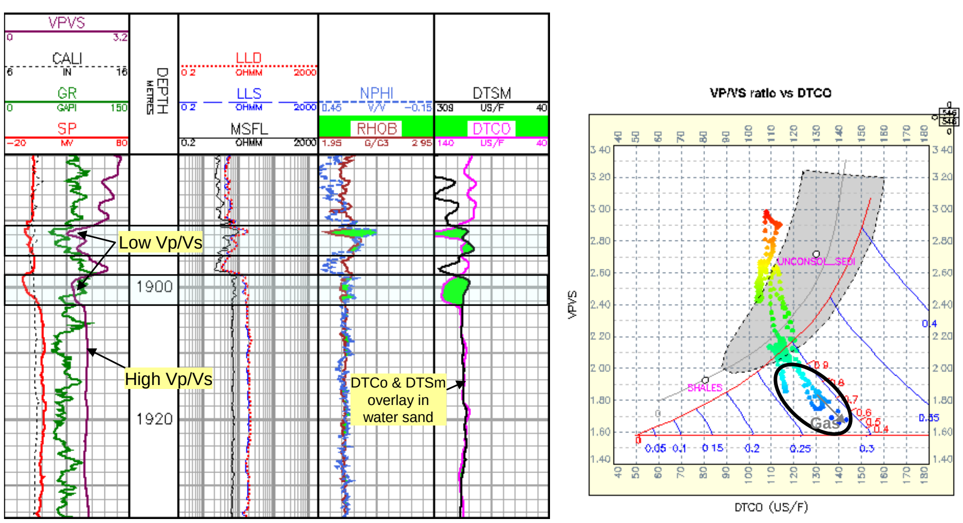

Figure-7: Well-F: DTCo & DTSm overlay and VpVs vs DTCo crossplot.